CrystEngComm

Accepted Manuscript

ROYAL SOCIETY OF CHEMISTRY

www.rsc.org/crystengcomm

Journal Name

RSCPublishing

COMMUNICATION

Effect of La/Gd ratios on phase, morphology, and fluorescence properties of $La_xGd_{1-x}F_3$: Nd^{3+} nanocrystals

Cite this: DOI: 10.1039/x0xx00000x

Chen Liang,[a] Zhongyue Wang,[a] Yanyan Zhang,[a] Weikuan Duan,[a] Weiyan Yue,[a] Yin Ding*[b] and Wei Wei*[c]

Received 00th January 2014,
Accepted 00th January 2014

DOI: 10.1039/x0xx00000x

www.rsc.org/

A series of $La_xGd_{1-x}F_3$:Nd^{3+} (x = 0~1) nanocrystals (NCs) were prepared via doping-controlled hydrothermal method. The XRD patterns show that orthorhombic phase of GdF_3 transforms into hexagonal phase of LaF_3 completely when x = 0.3, which is dramatically different with x = 0.5 for the bulk materials. Morphologies and near-infrared to near-infrared (NIR-to-NIR) fluorescence properties exhibit a direct dependence on the La/Gd ratio, providing an effective way to prepare numerous fluorescence NCs.

1. Introduction

GdF_3 is an excellent luminescent host matrix for various optically active lanthanide ions (Ln^{3+}) due to its low phonon energy and minimized quenching of the exited state of Ln^{3+}, which is favourable for attaining high fluorescence quantum efficiency.[1-3] So far, great efforts have been devoted to the synthesis methods for preparing lanthanide fluorides, such as decomposition of lanthanide organic precursors,[4-7] microwave and ionic liquid based synthesis method (ILs),[8-11] and hydrothermal/solvo-thermal method.[12-14] These methods, in spite of their significant contribution for optimizing the morphology and performance of lanthanide fluorides, still have their respective limitations. For instance, thermal decomposition of lanthanide trifluoroacetate precursors, the most widely-used method to prepare lanthanide fluorides with high monodispersity, should be carried out at a relatively high reaction temperature (>200 ^oC) under inert gas protection. Although the microwave and ILs methods have been successfully used in GdF_3 synthesis via a relatively green and facile route under mild conditions, they often require expensive equipments and reagents.

Hydro/ solvothermal method has been proven to be an effective and convenient process in preparing various inorganic nanomaterials, since its easily controllable reaction conditions, relatively high yield of the products, as well as frequently using environmental-friendly reagents (such as water, ethanol, et al) as the reaction medium.[12, 15] However, most GdF_3 nanocrystals (NCs) obtained by hydro/solvothermal method are composed of irregular particles in micrometre sizes.[12, 13] In order to obtain well-defined crystal phase and morphology of GdF_3 NCs, the hydro/solvothermal synthetic process generally imposed stringent control over a set of experimental parameters, such as surfactants, temperature, reaction time and concentration of precursors.[3, 14, 16] More importantly, most of the GdF_3 NCs obtained by these three synthetic methods crystallized in orthorhombic structure, which have been proved to be not as efficient as hexagonal phase with respect to fluorescent.[3]

At present, more attention is paid to the research on doping-controlled synthesis of lanthanide fluorides. Despite the widely investigated cubic to hexagonal phase transition in $NaYF_4$[17, 18] and $NaGdF_4$[19] by Ln^{3+}-doping, trigonal GdF_3 with 15 mol% La^{3+}-doping were also prepared.[20] Moreover, phase and morphology control of lanthanide fluorides were achieved via alkaline earth elements doping.[16, 21, 22] However, as far as we know, there have been few systematically studies focusing on the lanthanide doping-controlled synthesis of hexagonal GdF_3, neither research on fluorescence properties of GdF_3:Ln^{3+}.

In this communication, we have synthesized a series of undoped and Nd^{3+}-doped $La_xGd_{1-x}F_3$ NCs via a facile solvothermal method [see experimental details in supplementary information]. It is interesting that, by introducing high content of La^{3+} (30 mol%) into GdF_3, orthorhombic GdF_3 NCs are completely transformed into the hexagonal $La_{0.3}Gd_{0.7}F_3$ solid solutions, as far as we know, which have not been reported. Significantly, the morphology of these NCs turned to be nearly-monodispersed nanospheres with phase transformation from orthorhombic to hexagonal. Meanwhile, the near-infrared to near-infrared (NIR-to-NIR)

emissions of the Nd^{3+} doping into the NCs are greatly intensified by La^{3+}-doping.

2. Results and discussion

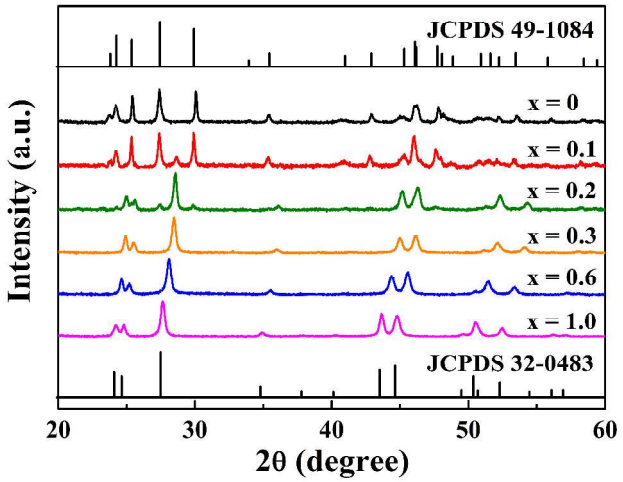

Fig. 1 XRD patterns of $La_xGd_{1-x}F_3$ (x = 0, 0.1, 0.2, 0.3, 0.6 and 1.0) NCs.

The X-ray powder diffractions (XRD) (Fig. 1) indicated that GdF_3 samples (x = 0) can be indexed to the standard card of orthorhombic GdF_3 (JCPDS 49-1804) without any impurity phase. With the increase of La^{3+} ions concentration, a gradual transformation from the orthorhombic phase of GdF_3 to the hexagonal phase of LaF_3 (JCPDS 32-0483) was observed, and 30% La^{3+} ions is sufficient for GdF_3 crystallizing in the LaF_3 hexagonal phase completely, which is dramatically different with 50% for the bulk materials.[23]

With further increase in La^{3+} ion concentration, no extra diffraction peaks were observed, indicating the formation of a homogeneous La-Gd solid solution.[17] At the same time, a slight peak shifts towards lower diffraction angles can be observed, which result from expansion in unit-cell volume owing to the substitution of Gd^{3+} (1.053Å) ions by larger La^{3+} (1.216Å) ions[24] in the host lattice with the increase of La^{3+}/Gd^{3+} ratio.[17]

Transmission Electron Microscopy (TEM) images (Fig. 2) showed that GdF_3 NCs exhibited a rod-like and somewhat irregular shape, and some of the rods tended to aggregate at one end. The selected area electron diffraction (SAED) pattern and the high-resolution TEM (HRTEM) image (Fig. 2 g) of the un-doped GdF_3 demonstrated the orthorhombic structure and single-crystalline nature of GdF_3 sample. With addition of La^{3+} ions (10 and 20 mol%), the anisotropic growth of these NCs weakened obviously, and the samples are mainly composed of irregular particles (Fig. 2 b, c).When La/Gd ratio reaches to 3/7, these NCs exhibit a spherical shape with an average diameter of ~50nm. The HRTEM image (Fig. 2 h) with clear lattice fringes indicates the crystallinity of the $La_{0.3}Gd_{0.7}F_3$ NCs. By further increasing La^{3+}/Gd^{3+} ratio (x = 0.3-1.0 mol%), the morphology of NCs had no significant change while the average size decreased gradually (Fig. 2 c-f), which is consistent with previous reports in the case of Eu^{3+}-doped $NaYF_4$[25] and Gd^{3+} doped $NaYF_4$[17].

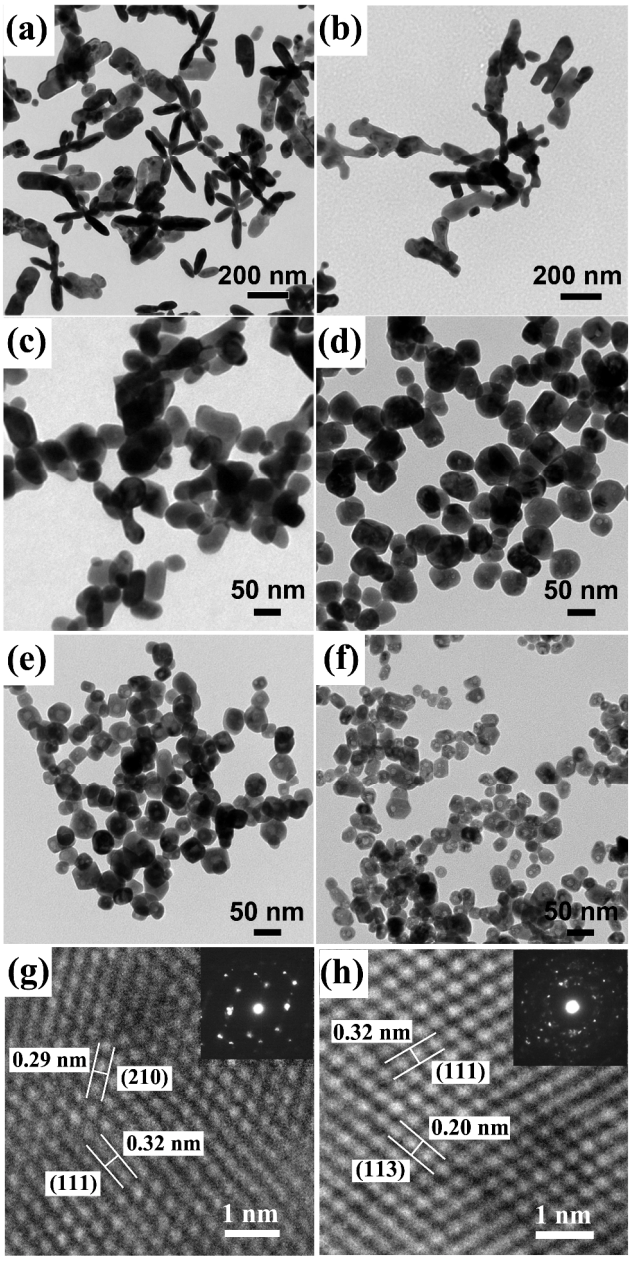

Fig. 2 (a)-(f), TEM images of $La_xGd_{1-x}F_3$ NCs obtained after 12 h hydrothermal treatment at 170 °C. (From a to f, x = 0, 0.1, 0.2, 0.3, 0.6 and 1.0). (g) and (h) are HRTEM images of (a) and (c), and the illustrations are SAED patterns of (a) and (c), respectively.

Crystal structure has been proved to be one of the most important factors that affect the growth behaviour of NCs.[13] When x = 0-0.3, the transition of two different phases can be found from the XRD patterns clearly as increasing La^{3+} concentration, which is supported by the observation of significant morphology changes in TEM images (Fig 2 a, b and c). By increasing La^{3+} concentrations (x>0.3), the products kept hexagonal phase, this may be the main reason for negligible changes in particle morphology. However, the particle size of

$La_xGd_{1-x}F_3$ (x = 0.3-1.0) NCs decreased gradually, which can be partly attributed to the effect of the La^{3+} dopant ions on crystal growth rate through surface charge modification.[17] With Gd^{3+} ions in the crystal lattice was replaced by La^{3+} ions, the surface electron charge density of NCs increased. Then the diffusion of negatively charged ions (F^-) to the surface was slowed down owing to an increase of charge repulsion and resulted in a reduction of the NCs size.

The transition of size and morphology for $La_xGd_{1-x}F_3$ NCs with increasing La^{3+} ions concentration was showed in Fig. 3.

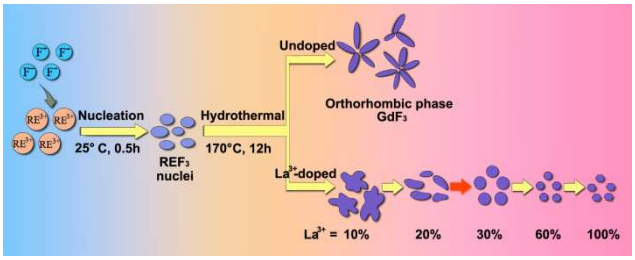

Fig. 3 Schematic illustration of the size and morphology transition of $La_xGd_{1-x}F_3$ NCs with La^{3+} ions concentration increasing.

We propose that the key reason for the crystalline transition from orthorhombic phase to the hexagonal phase of GdF_3 is the lowering of the energy barrier induced by dopant La^{3+}. It is known that the hexagonal phase is more thermodynamically stable than the orthorhombic phase of GdF_3.[26, 23] Thus, phase transition from orthorhombic to hexagonal can be achieved in two different ways. One of the methods is to provide enough energy to overcome the energy barrier between the orthorhombic and hexagonal phase, such as a high temperature up to 907.4°C.[23] The other method is to reduce the energy barrier between orthorhombic phase and hexagonal phase during the synthesis process.[18] As confirmed by previously reports, Ln^{3+} ions with larger ionic radius have lower energy barriers to the hexagonal phase products.[12, 13, 18] In our study, when the $La_xGd_{1-x}F_3$ NCs were synthesized, the dopant La^{3+} with larger ionic radius can decrease the energy barrier from orthorhombic to hexagonal transition, and tip the balance in favour of hexagonal phase GdF_3 during the process of crystal growth.

There is increasing interest in Nd^{3+}-doped NCs due to their NIR-to NIR stokes emission by ~800 nm excitation, which result in higher tissue depth, less thermal effect and significantly enhanced quantum yield (QY) than upconversion nanoparticles (UCNPs).[5, 27, 28] The fluorescence performance of dopant Ln^{3+} is tightly related to the environmental structure.[3, 17, 21] Hence, the phase conversion from orthorhombic to hexagonal phase may cause some interesting fluorescence for the dopant Nd^{3+}.

Photoluminescence properties of $La_xGd_{1-x}F_3:Nd^{3+}$ NCs were also investigated in these paper. Three emission peaks of $La_xGd_{1-x}F_3:Nd^{3+}$ (3 mol%) (x = 0, 0.1, 0.2, 0.3, 0.6 and 1.0) NCs centred at ~890 nm, ~1060 nm and ~1330 nm can be observed, which are assigned to the transitions of $^4F_{3/2} \rightarrow {}^4I_{9/2}$, $^4F_{3/2} \rightarrow {}^4I_{11/2}$, $^4F_{3/2} \rightarrow {}^4I_{13/2}$, respectively. The fluorescence intensity for the transition of $^4F_{3/2} \rightarrow {}^4I_{11/2}$ of increased firstly and then decreased with increasing La^{3+} ions concentrations (Fig. S1), and the sample with x = 0.2 exhibited the highest fluorescence intensity, which was about 3 times of that of $GdF_3:Nd^{3+}$ (x=0) NCs. To sum up, the photoluminescence properties of NCs are largely affected by factors such as the crystal structure, surface effect and morphology, et al.[29, 30] It has been reported that the fluorescence performance of hexagonal LaF_3 was superior to orthorhombic GdF_3.[3] As x changes from 0 to 0.3, crystal structure of $La_xGd_{1-x}F_3$ transforms from orthorhombic phase to hexagonal phase completely, and the morphologies of NCs changed significantly, which improve the fluorescence properties together. In the region of 0.3~1.0, crystalline phase and morphology of NCs did not change significantly, but the specific surface area increased with La^{3+} ions concentrations increasing (Tab. 1). Thus fluorescence quenching increased with increasing surface quenching centres. However, this issue will not be discussed in detail since it is complex and no final conclusion has yet been reached.[21, 31, 32]

Tab. 1 Measured Brunauer–Emmett–Teller (BET) and Langmuir surface areas of $La_xGd_{1-x}F_3$ (x=0-1) NCs.

x value	0	0.1	0.2	0.3	0.6	1.0
BET (m^2g^{-1})	10.25	12.34	13.08	17.75	28.19	32.50
Langmuir (m^2g^{-1})	13.98	17.59	17.68	24.20	38.58	43.87

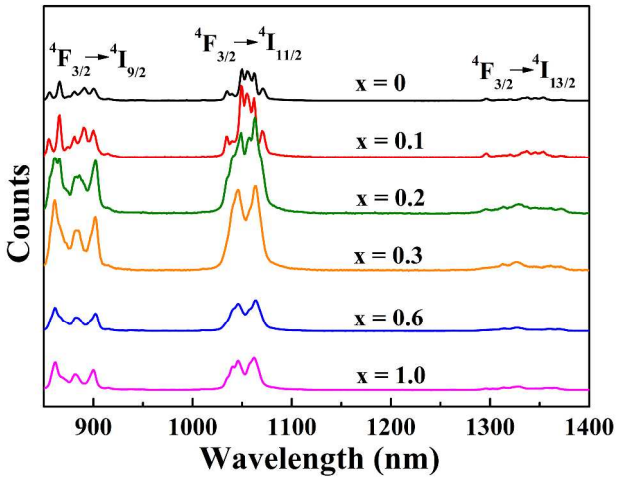

Fig. 4 Fluorescence spectra of $La_xGd_{1-x}F_3:Nd^{3+}$ (3 mol%) (x = 0, 0.1, 0.2, 0.3, 0.4, 0.6 and 1.0) NCs, measured at room temperature under 790 nm excitation.

The fluorescence lifetimes ($^4F_{3/2} \rightarrow {}^4I_{11/2}$ transition) of $La_xGd_{1-x}F_3:Nd^{3+}$ NCs (x = 0, 0.1, 0.2, 0.3, 0.6 and 1.0) had a similar variation trend with the fluorescence intensity (Fig. S2). Calculated by fitting the decay curves with double-exponential function, the lifetimes of $La_xGd_{1-x}F_3:Nd^{3+}$ NCs (x = 0, 0.1, 0.2, 0.3, 0.6 and 1.0) for $^4F_{3/2} \rightarrow {}^4I_{11/2}$ transition were determined as 95 μs, 128 μs, 222 μs, 210 μs,183 μs and 207 μs, respectively (Fig. 5).

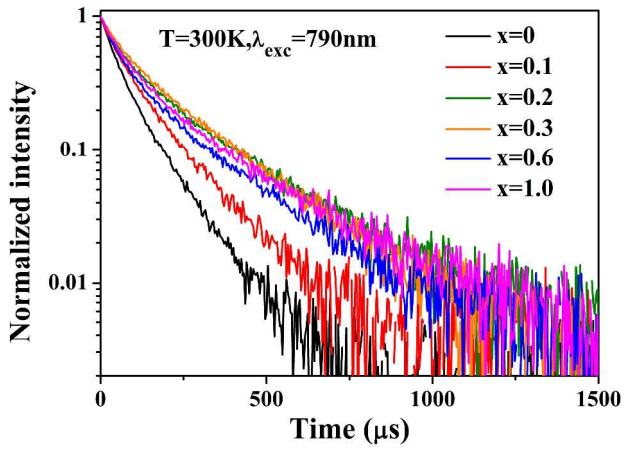

Fig. 5 Fluorescence decay curves of $La_xGd_{1-x}F_3:Nd^{3+}$ (3 mol%) NCs.

3. Conclusion

In summary, we have investigated the effect of La/Gd ratios on the crystal phase, morphologies and fluorescence properties of $La_xGd_{1-x}F_3$ NCs (x = 0~1). The orthorhombic GdF_3 transforms into hexagonal phase completely when x = 0.3, and $La_{0.2}Gd_{0.8}F_3:Nd^{3+}$ NCs exhibit the highest fluorescence intensity and longest lifetime for $^4F_{3/2}\rightarrow{}^4I_{11/2}$ transition. Considering both the excitation (790 nm) and emission (~890 nm, ~1060nm and ~1320nm) bands of these materials are in the "optical transparency window", as well as the intrinsic paramagnetic properties of Gd^{3+} ions, this doping-controlled sovolthermal method may open up an effective way to prepare various multi-function nano contrast agents. The research on magnetical properties and biomedical applications will be studied in the following work.

Acknowledgment

This work was financially supported by the National Basic Research Program of China (No. 2012CB933301) and National Natural Science Foundation of China (No. 60977023, 21105047, 61107015 and 61077070).

Notes and references

[a] Institute of Advanced Materials, Nanjing University of Posts and Telecommunications, Nanjing, Jiangsu, 210023, P.R. China.
[b] State Key Laboratory of Analytical Chemistry for Life Science, School of Chemistry and Chemical Engineering, Nanjing University, Nanjing, Jiangsu, 210093, P.R. China.
[c] School of Optoelectronic Engineering, Nanjing University of Posts and Telecommunications, Nanjing, Jiangsu, 210023, P.R. China.
Electronic Supplementary Information (ESI) available: [Experimental details and additional data]. See DOI: 10.1039/c000000x/

1. T. Grzyb, M. Runowski, A. Szczeszak and S. Lis, *J. Phys. Chem. C*, 2012, **116**, 17188.
2. H. X. Mai, Y. W. Zhang, R. Si, Z. G. Yan, L. D. Sun, L. P. You and C. H. Yan, *J. Am. Chem. Soc.*, 2006, **128**, 6426.
3. M. M. Lezhnina, T. Jüstel, H. Kätker, D. U. Wiechert and U. H. Kynast, *Adv. Funct. Mater.*, 2006, **16**, 935.
4. T. Paik, D. K. Ko, T. R. Gordon, V. Doan-Nguyen and C. B. Murray, *ACS nano*, 2011, **5**, 8322.
5. M. Pokhrel, L. C. Mimun, B. Yust, G. A. Kumar, A. Dhanale, L. Tang and D. K. Sardar, *Nanoscale*, 2014, **6**, 1667.
6. S. Mishra, S. Daniele, G. Ledoux, E. Jeanneauc and M. F. Joubert, *Chem. Commun.*, 2010, **46**, 3756.
7. S. Mishra, E. Jeanneau, A. L. Bulin, G. Ledoux, B. Jouguet, D. Amans, A. Belsky, S. Danieleb and C. Dujardin, *Dalton Trans.*, 2013, **42**, 12633.
8. H. Q. Wang and T. Nann, *Nanoscale Res. Lett.*, 2011, **6**, 267.
9. C. Lorbeer, J. Cybinska and A. V. Mudring, *Chem. Commun.*, 2010, **46**, 571.
10. S. Rodriguez-Liviano, N. O. Nuñez, S. Rivera-Fernández, J. M. de la Fuente and M. Ocaña, *Langmuir*, 2013, **29**, 3411.
11. M. He, P. Huang, C. L. Zhang, F. Chen, C. Wang, J. B. Ma, R. He and D. X. Cui, *Chem. Commun.*, 2011, **47**, 9510.
12. C. X. Li, J. Yang, P. P. Yang, H. Z. Lian and J. Lin, *Chem. Mater.*, 2008, **20**, 4317.
13. X. Wang, J. Zhuang, Q. Peng and Y. D. Li, *Inorg. Chem.*, 2006, **45**, 6661.
14. Y. Tian, H. Y. Yang, K. Li and X. Jin, *J. Mater. Chem.*, 2012, **22**, 22510.
15. D. Yang, X. Kang, M. Shang, G. Li, C. peng, C. Li and J. Lin, *Nanoscale*, 2011, **3**, 2589.
16. X. F. Wang, Y. Y. Bu, Y. Xiao, C. X. Kan, D. Lu and X. H. Yan, *J. Mater. Chem. C*, 2013, **1**, 3158.
17. F. Wang, Y. Han, C. S. Lim, Y. H. Lu, J. Wang, J. Xu, H. Y. Chen, C. Zhang, M. H. Hong and X. G. Liu, *Nature*, 2010, **463**, 1061.
18. X. F. Yu, M. Y. Li, M. Y. Xie, L. D. Chen, Y. Li and Q. Q. Wang, *Nano Res.*, 2010, **3**, 51.
19. C. Dong, J. Pichaandi, T. Regier and F. C. J. M. van Veggel, *J. Phys. Chem. C*, 2011, **115**, 15950.
20. C. Dong, M. Raudsepp and F. C. J. M. v. Veggel, *J. Phys. Chem. C*, 2009, **113**, 472.
21. D. Q. Chen, Y. L. Yu, F. Huang and Y. S. Wang, *Chem. Commun.*, 2011, **47**, 2601.
22. D. Q. Chen and Y. S. Wang, *Nanoscale*, 2013, **5**, 4621.
23. L. H. Brixner, M. K. Crawford, G. Hyatt, W. T. Carnall and G. Blasse, *J. Electrochem. Soc.*, 1991, **138**, 313.
24. R. D. Shannon, *Acta Cryst.*, 1976, **A32**, 751.
25. L. Y. Wang and Y. D. Li, *Chem. Mater.*, 2007, **19**, 727.
26. R. E. Thoma and G. D. Brunton, *Inorg. Chem.*, 1966, **5**, 1937.
27. U. Rocha, K. U. Kumar, C. Jacinto, I. Villa, F. Sanz-Rodríguez, M. del Carmen Iglesias de la Cruz, A. Juarranz, E. Carrasco, F. C. J. M. van Veggel, E. Bovero, J. G. Solé and D. Jaque, *Small*, 2013, 1.
28. G. Y. Chen, T. Y. Ohulchanskyy, S. Liu, W. C. Law, F. Wu, M. T. Swihart, H. Ågren and P. N. Prasad, *ACS nano*, 2012, **6**, 2969.
29. K. W. Krämer, D. Biner, G. Frei, H. U. Güdel, M. P. Hehlen and S. R. Lüthi, *Chem. Mater.*, 2004, **16**, 1244.
30. P. Ptacek, H. Schäfer, K. Kömpe and M. Haase, *Adv. Funct. Mater.*, 2007, **17**, 3843.
31. L. Zhu, Q. Li, X. D. Liu, J. Y. Li, Y. F. Zhang, J. Meng and X. Q. Cao, *J. Phys. Chem. C*, 2007, **111**, 5898.

32. G. F. Wang, Q. Peng and Y. D. Li, *J. Am. Chem. Soc.*, 2009, **131**, 14200.

A table of contents entry

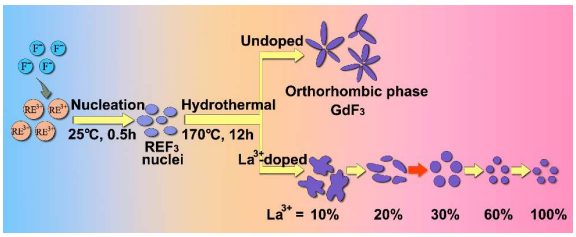

Phase transition from orthorhombic GdF_3 (nanorods) to nearly monodispersed hexagonal $La_{0.3}Gd_{0.7}F_3$ (nanospheres) solid solution was achieved by 30% La^{3+}-doping.